Hua-Long Jiang*, Song-Hao Jia, Da-Wei Zhou*, Chun-Ying Pu, Fei-Wu Zhang and Shuai Zhang

First-Principles Calculations of the Mechanical and Elastic Properties of $2H_c$- and $2H_a$-WS_2/CrS_2 Under Pressure

DOI 10.1515/zna-2015-0517
Received December 13, 2015; accepted March 30, 2016; previously published online May 3, 2016

Abstract: By utilizing the first-principles method, the pressure-induced effects on phase transition, mechanical stability, and elastic properties of WS_2/CrS_2 are investigated in the pressure range from 0 to 80 GPa. Transitions from $2H_c$ to $2H_a$ for WS_2 and CrS_2 are found to occur at 17.5 and 25 GPa, respectively. It is found that both $2H_a$ and $2H_c$ phases of WS_2 and CrS_2 meet the mechanical stability criteria up to 80 GPa, suggesting that those structures are mechanically stable. The bulk and shear modulus anisotropy of the two phases of WS_2 and CrS_2 decrease rapidly under pressure and, finally, trend to isotropy. With increasing pressure, the elastic moduli (Y, B, and G), sound velocities (v_s, v_p, v_m), and Debye temperatures (Θ) of $2H_a$ and $2H_c$ of WS_2 and CrS_2 increase monotonously. Moreover, the Debye temperature (Θ) of $2H_c$ phase is higher than that of $2H_a$ phase for both WS_2 and CrS_2. The bulk, shear, and Young's modulus, Poisson coefficient, and brittle/ductile behaviour are estimated. The percentages of anisotropy in compressibility and shear and the ratio of bulk to shear modulus (B/G) are also studied.

Keywords: CrS_2; Elastic Properties; First-Principles; Phase Transition; WS_2.

***Corresponding authors: Hua-Long Jiang and Da-Wei Zhou,** Department of Physics and Electronic Engineering, Nanyang Normal University, Nanyang 473061, China, E-mail: Jiang_hualong@163.com (H.-L. Jiang); zhoudawei@nynu.edu.cn (D.-W. Zhou)
Song-Hao Jia: Department of Computer Science and Information Technology, Nanyang Normal University, Nanyang 473061, China
Chun-Ying Pu and Shuai Zhang: Department of Physics and Electronic Engineering, Nanyang Normal University, Nanyang 473061, China
Fei-Wu Zhang: State Key Laboratory of Ore Deposit Geochemistry, Institute of Geochemistry, Chinese Academy of Sciences, Guiyang 550002, China; Nanochemistry Research Institute, Curtin University, Perth, WA 6845, Australia; and School of Mathematics and Physics, Suzhou University of Science and Technology, Suzhou 215009, China

1 Introduction

There is a growing interest in studding the structures and properties of two-dimensional transition metal dichalcogenides (TMDs) owing to their novel electronic and catalytic properties that differ from their bulk counterparts [1–3]. Because TMDs have in-plane covalent bonding and weak interlayer van der Waals interactions, they could be easily exfoliated down to a monolayer which shows very exotic properties. For example, the band-gap structure of MoS_2 shows an indirect-to-direct semiconductor transition from bulk to single-layer due to a lack of interlayer interaction [4, 5]. Two-dimensional dilute magnetic semiconductors are proposed for substitution of Mo by other transition metal atoms, such as W and Cr. Furthermore, TMDs also have shown exciting prospects for various applications, such as lubricants and catalysts in the petroleum industry [6], possible applications in optoelectronics and nanoelectronics [7], and energy-storage applications [8]. As an important member of TMDs, WS_2 has received a lot of attention. For example, WS_2 has been prepared into nanoparticles, nanotubes, nanoribbons, films, graphene-like WS_2, and WS_2 sheets [9–16]. Some features and properties of WS_2 such as tribological performance [10, 17, 18], structural, electronic [19], optical, and mechanical properties [4, 9, 20–24] have been studied. CrS_2 also attracted some researchers' interest, and the electronic properties [25, 26], optical, piezoelectric properties, and stability of this single-layer material were investigated and characterized [27].

However, most of the previous theoretical works focused on WS_2 and CrS_2 were carried out at 0 GPa. Very recently, high pressure in situ angle dispersive powder X-ray diffraction using synchrotron radiation together with high-pressure Raman analysis was performed on powder WS_2 samples to investigate the effect of pressure on crystal WS_2. However, it was reported that there was no phase transformations observed in WS_2 under compression for pressures up to 52 GPa [28]. As we have known, for most transition typical TMDs, there is a phase transition from $2H_c$ to $2H_a$ under pressure [29, 30]. As we know,

due to some reasons, such as the limitations of the experimental conditions, temperature effect, and higher phase transition barrier, some phase transition under pressure cannot be detected experimentally. So it is necessary to investigate structural evolution of WS_2 theoretically. Since chromium belongs to the same group as tungsten, we also investigate the possible pressure-induced transition from $2H_c$ to $2H_a$ for CrS_2.

In this paper, we first investigate the possible structural transitions of WS_2/CrS_2 under pressure, then study the anisotropy in elasticity and thermodynamic properties of them under pressure. We found that both CrS_2 and WS_2 will transform from $2H_c$ to $2H_a$ phase under pressure, and the anisotropy in elasticity and thermodynamic properties of $2H_c$ and $2H_a$ phases for both WS_2/CrS_2 are calculated and compared.

The paper is structured as follows. Section 2 contains the computational details. The results and discussion are provided in Section 3. Finally, we present our conclusions in Section 4.

2 Computational Methods

The calculations reported in this work were performed using the CASTEP code in the Materials Studio software [31, 32]. The density functional theory of the plane-wave pseudopotential method [33] was used to perform geometry optimisation and calculate the elastic parameters. The exchange and correlation functional were treated by the local density approximation [34, 35]. The plane-wave cutoff energy of 800 eV was used for the all structures studied in this work. The k integration over the Brillouin zone was performed up to a $14\times14\times4$ Monkhorst–Pack [36] mesh. Coulomb potential energy caused by electron–ion interaction is described using Norm-Conserving Pseudopotential [37]. In order to make our calculations standard, energy-difference threshold for the convergence is taken as $5*10^{-6}$ eV/atom. These values ensure a satisfactory convergence, and thus provide reliable results.

3 Results and Discussion

The two typical structures of TMDs ($2H_c$ and $2H_a$) [29] are shown in Figure 1, and the pressure-induced sliding of layers was reported to be responsible for the transition from $2H_c$ to $2H_a$ structure [29]. The calculated lattice constants of $2H_c$ structures for both CrS_2 and WS_2 at zero pressure together with other theoretical values are listed in Table 1, and our results agree well with other reference's data. These guarantee the reliability of our calculation.

To investigate the possible pressure-induced structural transition of CrS_2 and WS_2, we applied hydrostatic pressure to $2H_c$ and $2H_a$ phases, and then fully optimised the lattice parameters and atomic positions. Figure 2a and b plot the relative enthalpy versus pressure for the $2H_c$ and $2H_a$ structures of CrS_2 and WS_2, respectively. For CrS_2,

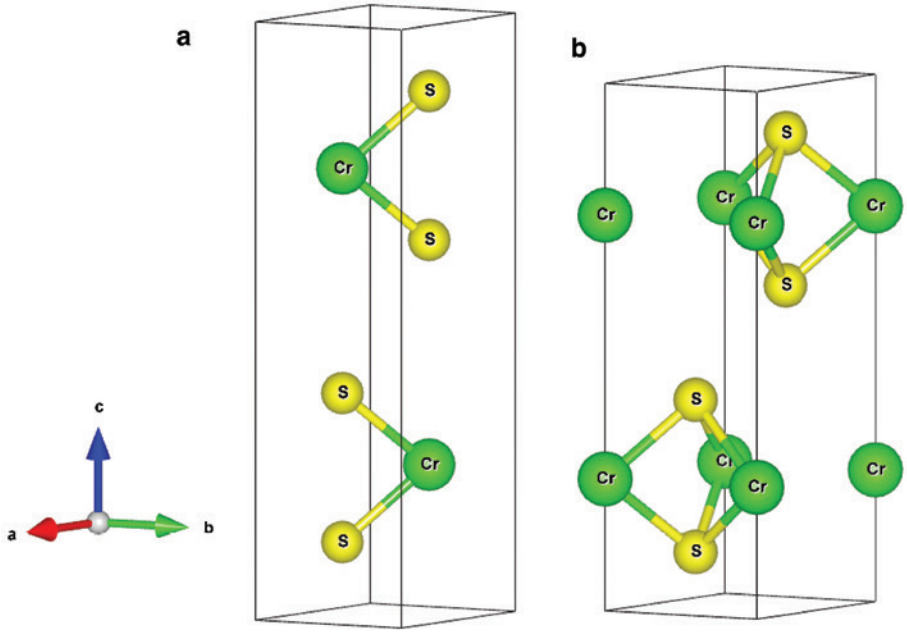

Figure 1: (a) Structures of $2H_c$-XS_2 (X = W, Cr). (b) Structures of $2H_a$-XS_2 (X = W, Cr).

Table 1: Calculated lattice constant *a* (Å) at zero pressure, together with this work and other references for comparison.

	Reference	Lattice constant *a*/Å	Lattice constant *c*/Å
WS_2	This work	3.1462	12.163
	[38]	3.1532	12.323
	[39]	3.154	12.362
CrS_2	This work	3.04	14.409
	[40]	3.06	
	[41]	3.05	

$2H_a$ structure is with lower enthalpy than $2H_c$ structure for pressures ≥17.5 GPa. For WS_2, enthalpy of $2H_a$ phase is lower than that of $2H_c$ phase at 25 GPa. So, for CrS_2 and WS_2, the phase-transition pressures for $2H_c$ to $2H_a$ phase are 17.5 and 25 GPa, respectively.

The elastic properties of a material are very important for understanding and predicting the mechanical stability, and for indications of material-related properties such as brittleness, ductility, based on the analysis of elastic constants C_{ij}, bulk modulus B, and shear modulus G. The elastic constants can be obtained by calculating the stress response when a small strain was forced to the optimised unit cell [42]. According to the strain energy theory, for a mechanically stable structural phase, the strain energy should be positive, and the matrix of elastic constants should be positive, definite, and symmetrical [43]. For hexagonal structure, the mechanical stability criterion can be expressed as [44]:

$$C_{11}>0,\ C_{44}>0,\ C_{11}-C_{12}>0,\ (C_{11}+C_{12})\,C_{33}-2C_{13}^2>0. \tag{1}$$

According to the calculated elastic constants of the hexagonal $2H_c$ and $2H_c$ phase of CrS_2 and WS_2, it is found that they all satisfy their stability conditions up to 80 GPa. That means, for CrS_2 and WS_2, both the $2H_a$ and $2H_c$ hexagonal phases are mechanically stable up to 80 GPa. In the view of mechanical stability criteria, $2H_c$ phase may exist as metastable structure at higher pressure.

The changes of the elastic constants with pressure for both CrS_2 and WS_2 are presented in Figures 3 and 4, respectively. It can be found that the elastic constants C_{11} and C_{33} increase quickly and monotonically with pressure, while the elastic constants C_{44}, C_{12}, and C_{13} increase comparatively slowly. For these two materials, C_{11} and C_{33} are larger than other elastic constants, which indicate that they are very incompressible under uniaxial stress along x (ε11) or z (ε33) axis.

Bulk modulus reflects the compressibility of the solid under hydrostatic pressure. The bulk modulus (B) and shear modulus (G) can be estimated according to the Voigt–Reuss–Hill approximation [45–48]. For the hexagonal systems, they can be calculated with the computed data using the following relations:

$$C_{66}=(C_{11}-C_{12})/2, \tag{2}$$

$$B_V=\frac{1}{9}(2(C_{11}+C_{12})+C_{33}+4C_{13}), \tag{3}$$

$$B_R=\frac{(C_{11}+C_{12})C_{33}-C_{13}^2}{C_{11}+C_{12}+2C_{33}-4C_{13}}, \tag{4}$$

$$G_V=\frac{1}{30}(C_{11}+C_{12}+2C_{33}-4C_{13}+12C_{44}+12C_{66}), \tag{5}$$

$$G_R=\frac{5}{4}\frac{((C_{11}+C_{12})C_{33}-C_{13}^2)^2C_{44}C_{66}}{3B_VC_{44}C_{66}+((C_{11}+C_{12})C_{33}-C_{13}^2)^2(C_{44}+C_{66})}, \tag{6}$$

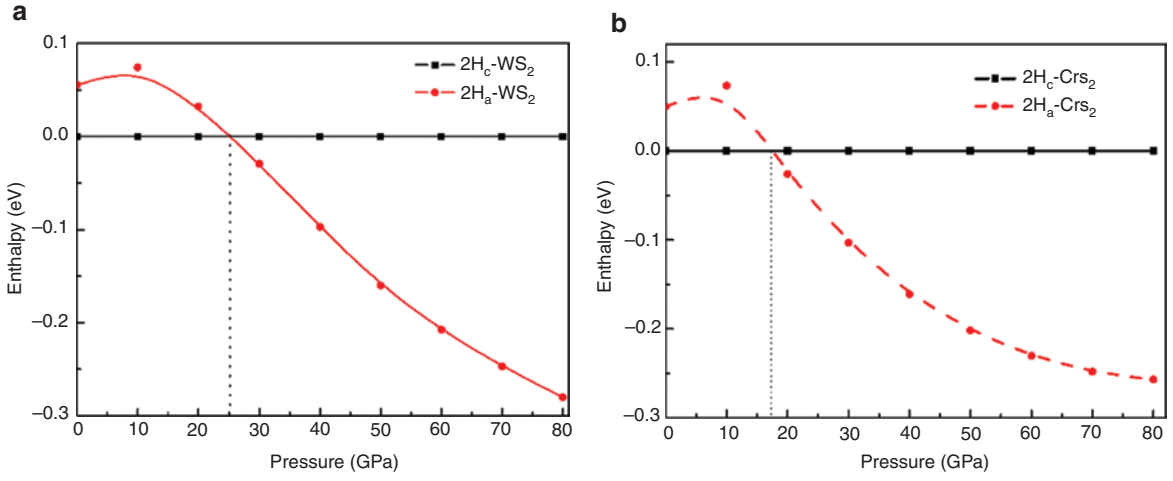

Figure 2: (a) Enthalpy versus pressure for the $2H_c$ and $2H_a$ structures of WS_2. (b) Enthalpy versus pressure for the $2H_c$ and $2H_a$ structures of CrS_2.

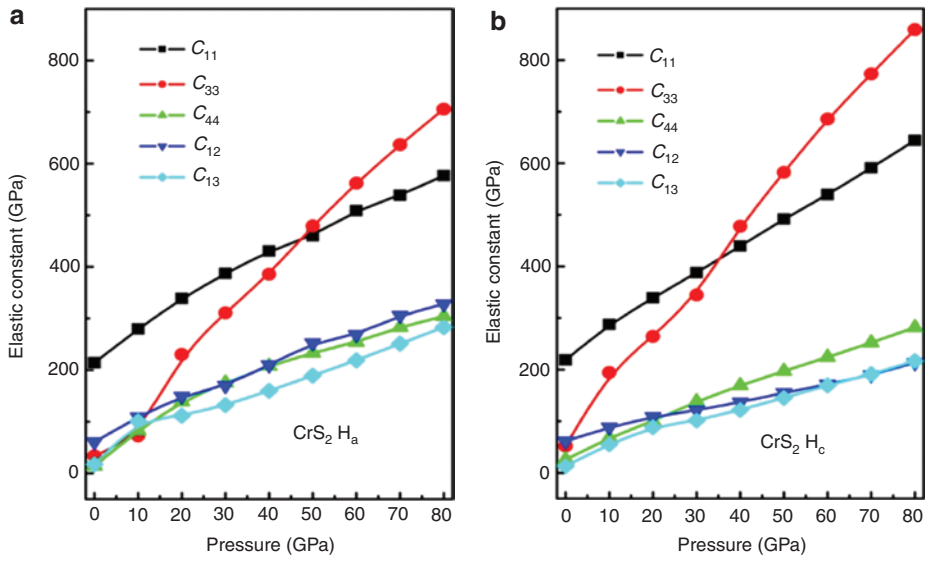

Figure 3: (a) Elastic constants of $2H_a$ phase of CrS_2 as a function of pressure. (b) Elastic constants of $2H_c$-phase of CrS_2 as a function of pressure.

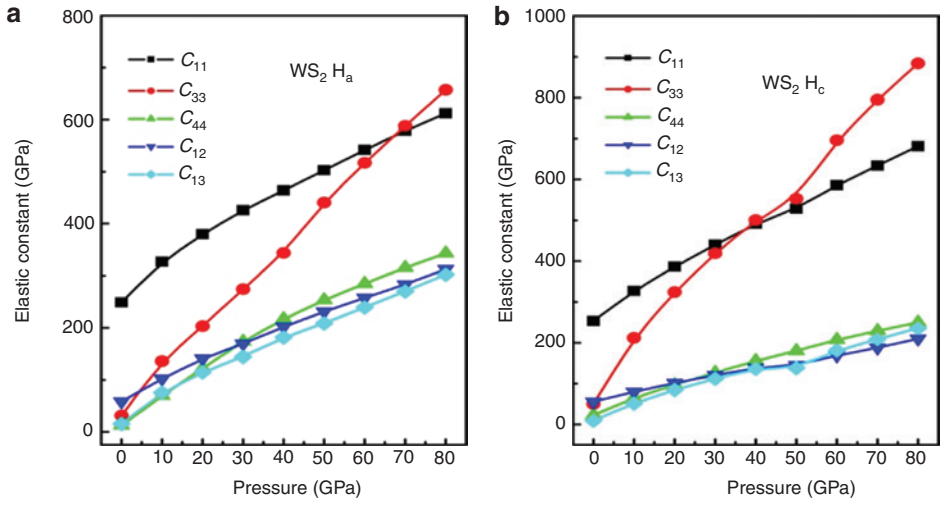

Figure 4: (a) Elastic constants of $2H_c$ phase of WS_2 as a function of pressure. (b) The elastic constants of $2H_a$ phase of WS_2 as a function of pressure.

$$B=(B_V+B_R)/2, \tag{7}$$

$$G=(G_V+G_R)/2. \tag{8}$$

The elastic anisotropy of crystals has a great impact on the properties of physical mechanism, such as anisotropic plastic deformation, elastic instability, and crack behavior. Hence, it is important to calculate the elastic anisotropy to improve its mechanical durability. The universal anisotropic index (A^U) is represented as

$$A^U=5\frac{G_V}{G_R}+\frac{B_V}{B_R}-6. \tag{9}$$

The percentage elastic anisotropy in compressibility and shear can be used as follows:

$$A_B=\frac{B_V-B_R}{B_V+B_R}, \tag{10}$$

$$A_G=\frac{G_V-G_R}{G_V+G_R}, \tag{11}$$

where B and G denote the bulk and shear modulus, and the subscripts V and R represent the Voigt and Reuss bounds. For these two formulas, a value of zero is associated with

isotropic elastic constants, while a value of 1 (100 %) is the largest possible anisotropy. The calculated anisotropic index and percent anisotropy factors are shown in Tables 2 and 3, respectively. It can be seen that the two phases of WS_2 and CrS_2 are anisotropic under the ordinary condition. With increasing pressure, the calculated universal anisotropic index (A^U) decreases. So, both the anisotropies of $2H_a$- and $2H_c$-WS_2 and CrS_2 decrease with pressure. Furthermore, the results also indicate that the $2H_a$ phase of WS_2 and CrS_2 has stronger mechanical anisotropy than the $2H_c$ phase. The value of bulk modulus anisotropy and shear modulus anisotropy decreases first, and they will be close to zero under certain pressure (such as the value of A_B of $2H_a$-WS_2 under 70 GPa). So, as the pressure increases, the bulk modules and shear modulus of two structural of WS_2 and CrS_2 become slightly anisotropic and, finally, turn to isotropic under certain pressures.

Debye temperature is closely related to many physical properties of solids, such as specific heat, stability of lattices, and melting temperature. At low temperature, it can be calculated using the average sound velocity (v_m) according to the following [49]:

$$\Theta=\frac{h}{k}\left(\frac{3n}{4\pi V}\right)^{\frac{1}{3}} v_m, \tag{12}$$

where h is the Plank's constant, k is the Boltzmann's constant, and V is the atomic volume. The average sound velocity (v_m) in the polycrystalline material can be obtained using the following [49]:

$$v_m=\left[\frac{1}{3}\left(\frac{2}{v_s^3}+\frac{1}{v_p^3}\right)\right]^{-\frac{1}{3}}, \tag{13}$$

where v_s and v_p are the transverse and longitudinal sound velocity, and are given by Navier's equation [49]:

$$v_s=\sqrt{G/\rho}, \tag{14}$$

$$v_p=\sqrt{(B+4G/3)/\rho}. \tag{15}$$

Depending upon the above equations, the average sound velocity and Debye temperature of $2H_c$- and $2H_a$-WS_2/CrS_2 are calculated and listed in Tables 2 and 3, respectively. It can be seen that v_m and Θ of $2H_c$- and

Table 2: Anisotropic factors, Debye temperature, average sound velocity of $2H_c$, and $2H_a$-WS_2.

Pressure (Gpa)	WS_2 ($2H_a$ phase)							WS_2 ($2H_c$ phase)						
	B	G	A^U	A_B	A_G	V_m	Θ	B	G	A^U	A_B	A_G	V_m	Θ
0	54	37	9.111	0.4519	0.4273	2428	277	60	48	4.382	0.3105	0.2583	2729	313
10	130	81	0.815	0.1009	0.0558	3353	401	133	91	0.547	0.0275	0.0468	3557	425
20	179	108	0.438	0.0544	0.0313	3743	458	181	120	0.174	0.0048	0.0162	3950	482
30	220	135	0.407	0.0278	0.0339	4062	506	220	145	0.062	0.0004	0.0061	4233	525
40	263	152	0.518	0.0133	0.0468	4235	535	256	168	0.021	0.0000	0.0022	4463	561
50	303	173	0.521	0.0034	0.0489	4430	566	271	189	0.010	0.0000	0.0010	4633	590
60	341	189	0.590	0.0007	0.0557	4565	590	324	213	0.027	0.0036	0.0020	4847	624
70	376	204	0.679	0.0000	0.0637	4676	610	361	232	0.043	0.0065	0.0030	4991	649
80	412	215	0.790	0.0003	0.0733	4750	625	397	250	0.057	0.0085	0.0039	5112	671

Table 3: Anisotropic factors, Debye temperature, average sound velocity of $2H_c$, and $2H_a$-CrS_2.

Pressure (GPa)	CrS_2 ($2H_a$ phase)							CrS_2 ($2H_c$ phase)						
	B	G	A^U	A_B	A_G	V_m	Θ	B	G	A^U	A_B	A_G	V_m	Θ
0	52	34	6.168	0.3898	0.3284	3782	448	58	44	2.879	0.2663	0.1772	4258	508
10	99	51	7.419	0.3973	0.3789	4326	540	126	83	0.261	0.0256	0.0204	5487	682
20	178	107	0.354	0.0262	0.0292	5962	764	166	106	0.060	0.0095	0.0041	5997	763
30	214	131	0.327	0.0103	0.0297	6429	838	195	134	0.013	0.0029	0.0008	6542	848
40	254	146	0.455	0.0051	0.0426	6663	881	235	162	0.019	0.0003	0.0019	7022	925
50	295	155	0.688	0.0008	0.0643	6747	903	272	186	0.044	0.0022	0.0040	7372	984
60	332	174	0.581	0.0000	0.0549	7037	952	307	208	0.076	0.0054	0.0065	7669	1035
70	369	182	0.836	0.0005	0.0771	7113	971	341	231	0.096	0.0070	0.0081	7953	1085
80	404	195	0.848	0.0016	0.0779	7267	1001	379	253	0.120	0.0082	0.0103	8210	1130

$2H_a$-WS_2/CrS_2 increase with increasing pressure. Additionally, the calculated results predict that Θ of $2H_c$ phase is higher than that of $2H_a$ phase for both WS_2 and CrS_2.

Knowing G and B, the Young's modulus Y and Poisson's ratio δ, which are frequently measured for polycrystalline materials when investigating their hardness, can be calculated from the isotropic relations:

$$Y=\frac{9GB}{3B+G}, \tag{16}$$

$$\delta=\frac{3B-2G}{2(3B+G)}. \tag{17}$$

The pressure dependencies of Young's modulus Y and shear modulus G of CrS_2 and WS_2 at various pressures are plotted in Figure 5a and b, respectively. It can be seen that both $2H_c$ and $2H_a$ phases of CrS_2 and WS_2 show similar trends under pressure. The values of G and Y increase with increasing pressure, and both of them were affected significantly by the pressure. Furthermore, it is noted from Figure 5 that G and Y change approximately linearly with the pressure, and the values of G and Y of $2H_c$ phase are larger than that of $2H_a$ phase for both CrS_2 and WS_2.

Poisson's ratio δ is related to the volume change during elastic deformation [50]. It can be used to assess the stability of a crystal against shear. The range of values for Poisson's ratio is –1 to 0.5, with –1 indicating the material does not change its shape and 0.5 indicating the volume remains unchanged during elastic deformation. The obtained Poisson's ratio for $2H_c$- and $2H_a$-CrS_2 at pressure 0–80 GPa are 0.194–0.227 and 0.23–0.29, respectively, which indicate that both $2H_c$- and $2H_a$-CrS_2 have central interatomic forces and are relatively stable against shear. As shown in Figure 6a, the Poisson's ratio δ of $2H_c$- and $2H_a$-CrS_2 increases with increasing pressure, and $2H_a$ phase has larger δ than $2H_c$ phase. The changes of δ with pressure for $2H_c$- and $2H_a$-WS_2 are shown in Figure 6b, and it can be seen that the change trends of δ are similar with that of CrS_2.

Considering that the bulk modulus B represents the resistance to fracture, while the shear modulus G represents the resistance to plastic deformation, the ratio of bulk to shear modulus (B/G) was introduced to measure the empirical malleability of polycrystalline materials [51]. The value at the critical point which separates ductile and brittle materials is about 1.75. If $B/G>1.75$, a material behaves in a ductile manner, and if not, a material will demonstrate brittleness. Higher (lower) values of B/G mean higher ductile (brittle) of a material. The B/G ratios of the two phases of CrS_2 at pressure from 0 to 80 GPa are shown in Figure 6a, and it is found that with increasing pressure, the B/G value of $2H_c$ phase increases from 1.30 to 1.49, while the B/G value of $2H_a$ phase increases from 1.53 to 2.07. Therefore, the $2H_c$ phase of WS_2 is brittle over the pressure range of 0–80 GPa, while $2H_a$ phase changes from brittle to ductile with increasing pressure. Similar features are also found in the B/G ratios of WS_2. The B/G ratios of WS_2 of the two phases at pressure from 0 to 80 GPa are shown in Figure 6b; with increasing pressure, the B/G value of $2H_c$ phase increases from 1.24 to 1.58, while the B/G value of $2H_a$ phase increases from 1.45 to 1.91. Therefore, the $2H_c$ phase of WS_2 is brittle up to 80 GPa, while the $2H_a$ phase changes from brittle to ductile with pressure increasing.

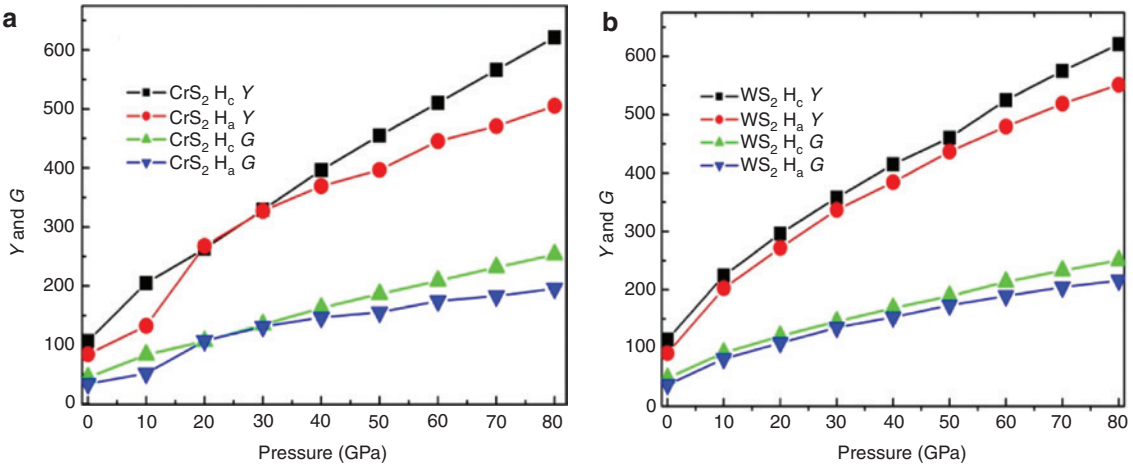

Figure 5: (a) Pressure dependencies of the shear modulus G and Young's modulus Y of CrS_2. (b) Pressure dependencies of the shear modulus G and Young's modulus Y of WS_2.

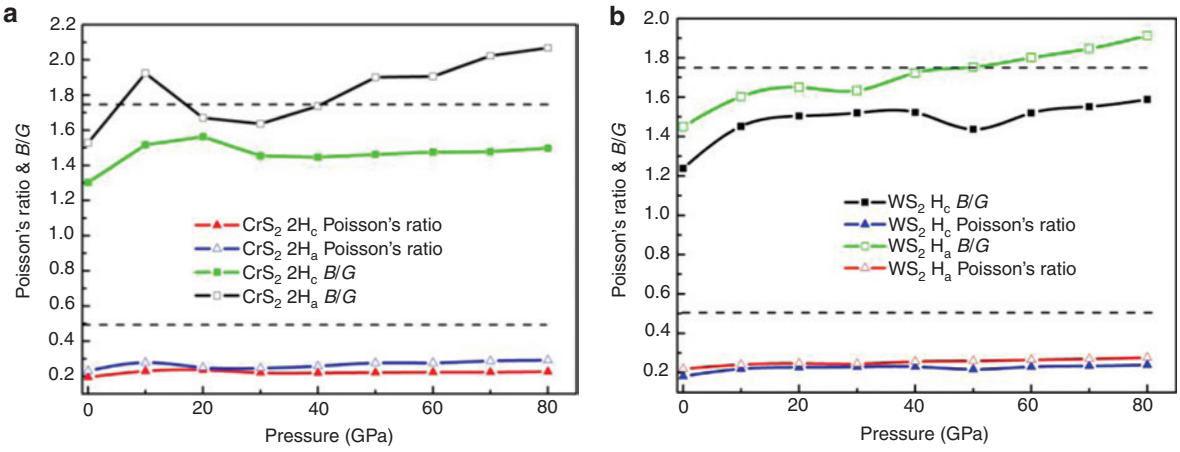

Figure 6: (a) Pressure dependencies of the Poisson's ratio and the ratio of bulk to shear modulus (B/G) of CrS_2. (b) Pressure dependencies of the Poisson's ratio and the ratio of bulk to shear modulus (B/G) of WS_2.

4 Conclusions

In this work, the pressure-induced phase transition, mechanical stability, and elastic properties of $2H_c$- and $2H_a$-WS_2/CrS_2 are investigated using the first-principles method. The calculated equilibrium lattice parameters of $2H_c$-WS_2/CrS_2 at 0 GPa are well in agreement with the experimental and other theoretical values. Although the transition for $2H_c$ to $2H_a$ phase was not observed experimentally for WS_2, we found that CrS_2 and WS_2 will transform from $2H_c$ to $2H_a$ phase at 17.5 and 25 GPa, respectively. According to the mechanical stability criterion, both $2H_c$- and $2H_a$-WS_2/CrS_2 exhibit mechanical stability in the pressure range of 0–80 GPa. The shear modulus, Young's modulus, Debye temperature, and average sound velocity of $2H_c$- and $2H_a$-WS_2/CrS_2 increase with the increasing pressure. The changes of Poisson's ratio and ratio of bulk to shear modulus (B/G) are also studied, and our results show that the $2H_c$ phase of WS_2/CrS_2 is brittle on the whole pressure range we investigated, while the $2H_a$ phase changes from brittle to ductile with pressure increasing. We also found that the two phases of WS_2 and CrS_2 are anisotropic under the ordinary condition, while the mechanical anisotropy of $2H_a$- and $2H_c$-WS_2 and CrS_2 decreases as pressure increases.

Acknowledgments: This work was supported by the Natural Science Foundation of China (Grant Nos. U1304612, U1404608, and 51501093), Young Core Instructor Foundation of Henan Province (Grant No. 2015GGJS-122), Science Technology Innovation Talents in Universities of Henan Province (Grant No. 16HASTIT047), Innovation Scientists and Technicians Troop Construction Projects of Henan Province (Grant No. C20150029), and Scientific Research Fund of Henan Provincial Education Department (Grant No. 15B140006). Feiwu Zhang acknowledges the support of the Thousand Young Talents Program and the Hundred Talent Program of the Chinese Academy of Sciences.

References

[1] Y. Li, Z. Zhou, S. Zhang, and Z. Chen, J. Am. Chem. Soc. **130**, 16739 (2008).
[2] K. F. Mak, C. Lee, J. Hone, J. Shan, and T. F. Heinz, Phys. Rev. Lett. **105**, 136805 (2010).
[3] A. Splendiani, L. Sun, Y. Zhang, T. Li, J. Kim, et al., Nano Lett. **10**, 1271 (2010).
[4] Y. Ding, Y. Wang, J. Ni, L. Shi, S. Shi, et al., Phys. B **406**, 2254 (2011).
[5] S. Lebègue and O. Eriksson, Phys. Rev. B **79**, 5409 (2009).
[6] P. Raybaud, J. Hafner, G. Kresse, and H. Toulhoat, J. Phys. Condens. Matter **9**, 11107 (1997).
[7] Q. Wang, K. Kalantar-Zadeh, A. Kis, J. Coleman, and M. Strano, Nat. Nanotech. **7**, 699 (2012).
[8] M. Chhowalla, H. S. Shin, G. Eda, J. L. Li, K. P. Loh, et al., Nat. Chem. **5**, 263 (2013).
[9] A. Kumar and P. K. Ahluwalia, Eur. Phys. J. B **85**, 186 (2012).
[10] C. Drummond, N. Alcantar, J. Israelachvili, R. Tenne, and Y. Golan, Adv. Funct. Mater. **11**, 348 (2001).
[11] W. Ho, J. C. Yu, J. Lin, J. G. Yu, and P. Li, Langmuir **20**, 5865 (2004).
[12] A. K. M. Newaz, D. Prasai, J. I. Ziegler, D. Caudel, S. Robinson, et al., Solid State Commun. **155**, 49 (2013).
[13] K. K. Kam and B. A. Parklnson, J. Phys. Chem. **86**, 463 (1982).
[14] Z. Wang, K. Zhao, H. Li, Z. Liu, Z. Shi, et al., J. Mater. Chem. **21**, 171 (2011).
[15] H. S. S. Ramakrishna Matte, A. Gomathi, A. K. Manna, D. J. Late, R. Datta, et al., Angew. Chem. **122**, 4153 (2010).
[16] M. Nath, A. Govindaraj, and C. N. R. Rao, Adv. Mater. **13**, 283 (2001).
[17] S. V. Prasad and J. S. Zabinski, J. Mater. Sci. Lett. **12**, 1413 (1993).

[18] L. F. Mattheis, Phys. Rev. Lett. **30**, 784 (1973).
[19] G. Arora, Y. Sharma, V. Sharma, G. Ahmed, S. K. Srivastava, et al., J. Alloys Compd. **470**, 452 (2009).
[20] I. Kaplan-Ashiri and R. Tenne, J. Clus. Sci. **18**, 549 (2007).
[21] A. Kuc, N. Zibouche, and T. Heine, Phys. Rev. B **83**, 245213 (2011).
[22] H. Jiang, J. Phys. Chem. C **116**, 7664 (2012).
[23] T. Björkman, A. Gulans, A. V. Krasheninnikov, and R. M. Nieminen, Phys. Rev. Lett. **108**, 235502 (2012).
[24] L. P. Feng, Z. Q. Wang, and Z. T. Liu, Solid State Commun. **187**, 43 (2014).
[25] S. Lebègue, T. Björkman, M. Klintenberg, R. M. Nieminen, and O. Eriksson, Phys. Rev. X **3**, 031002 (2013).
[26] C. Ataca, H. Sahin, and S. Ciraci, J. Phys. Chem. C **116**, 8983 (2012).
[27] H. L. Zhuang, M. D. Johannes, M. N. Blonsky, and R. G. Hennig, Appl. Phys. Lett. **104**, 022116 (2014).
[28] N. Bandaru, R. S. Kumar, J. Baker, O. Tschauner, T. Hartmann, et al., Int. J. Mod. Phys. B **28**, 134 (2014).
[29] L. Hromadová, R. Martoňák, and E. Tosatti, Phys. Rev. B **87**, 144105 (2013).
[30] N. Bandaru, R. S. Kumar, D. Sneed, O. Tschauner, J. Baker, et al., J. Phys. Chem. C **118**, 3230 (2014).
[31] S. J. Clark, M. D. Segall, C. J. Pickard, P. J. Hasnip, M. J. Probert, et al., Z. Kristallogr. **220**, 567 (2005).
[32] M. D. Segall, P. J. D. Lindan, M. J. Probert, C. J. Pickard, P. J. Hasnip, et al., J. Phys. Condens. Matter **14**, 2717 (2002).
[33] P. Hohenberg and W. Kohn, Phys. Rev. B **136**, 864 (1964).
[34] D. M. Ceperley and B. J. Alder, Phys. Rev. Lett. **45**, 566 (1980).
[35] J. P. Perdew and A. Zunger, Phys. Rev. B **23**, 5048 (1981).
[36] H. J. Monkhorst and J. D. Pack, Phys. Rev. B **13**, 5188 (1976).
[37] D. R. Hamann, M. Schluter, and C. Chiang, Phys. Rev. Lett. **43**, 1494 (1979).
[38] C. Lee, J. Hong, M. H. Whangbo, and J. H. Shim, Chem. Mater. **25**, 3745 (2013).
[39] A. Matthäus, A. Ennaoui, S. Fiechter, S. Tiefenbacher, T. Kiesewetter, et al., J. Electrochem. Soc. **144**, 1013 (1997).
[40] X. L. Wei, H. Zhang, G. C. Guo, X. B. Li, W. M. Lau, et al., J. Mater. Chem. A **2**, 2101 (2014).
[41] H. Guo, N. Lu, L. Wang, X. Wu, and X. C. Zeng, J. Phys. Chem. C **118**, 7242 (2014).
[42] B. B. Karki, L. Stixrude, S. J. Clark, M. C. Warren, G. J. Ackland, et al., Am. Mineral. **82**, 51 (1997).
[43] M. H. Sadd, Elasticity: Theory, Applications, and Numerics, 2nd ed., Academic Press, Burlington, MA 2009.
[44] G. V. Sin'Ko and N. A. Smirnov, J. Phys.: Condens. Matter. **14**, 6989 (2002).
[45] W. Voigt, Lehrbuch der kristallphysik: Teubner-Leipzig, Macmillan, New York 1928.
[46] A. Reuss and Z. Angew, Math. Mech. **9**, 55 (1929).
[47] R. Hill, Proc. Phys. Soc. London, Sect. A **65**, 349 (1952).
[48] X. H. Deng, W. Lu, Y. M. Hu, and H. S. Gu, Phys. B **404**, 1218 (2009).
[49] O. L. Anderson, J. Phys. Chem. Solids **24**, 909 (1963).
[50] P. Ravindran, L. Fast, P. A. Korzhavyi, B. Johansson, J. Wills, et al., J. Appl. Phys. **84**, 4891 (1998).
[51] S. F. Pugh, Philos. Mag. **45**, 823 (1954).